UNIVERSITY OF WEST BOHEMIA

Applied and Computational Mechanics 1 (2007) 667 - 676

Applied and Computational Mechanics

Form of growth law

M. Tringelová[a,*]

[a] *Faculty of Applied Sciences, UWB in Pilsen, Univerzitní 22, 306 14 Plzeň, Czech Republic*

Received 10 September 2007; received in revised form 10 October 2007

Abstract

Our aim in future is to computer simulate the mechanical stimulated postnatal heart development (normal growth, heart hypertrophy, etc.). We are now interested in the study of the form of growth law [1], which we could use for the simulation. We follow the theory of volumetric growth in [1]. This theory is based on the theory of generalized continuum [2] and describes the volumetric growth of tissue from macroscopic point of view.

Keywords: growth law, continuum mechanics, added degree of freedom, mechanical load, ventricle

1. Introduction

The heart is compound from four chambers, two of them are thick walled ventricles - right and left ventricle. Due to the different changes in haemodynamics during the pumping function becomes the left ventricle bigger and thicker than the right ventricle, after birth on. This difference is a sufficient example of soft tissue adaptation to the change in applied both volume and pressure load. We summarize volume and pressure overload in the second section.

We would like to apply the theory of volumetric growth in [1], based on the theory of generalized continuum in [2], to the computer simulation of ventricle adaptation to the mechanical load, after birth on. This theory takes into account microstructure of tissue from macroscopic point of view, thanks the addition of other degree of freedom. We will discuss the main idea of this theory in the third section. We refer the readers to the article [1] to better understanding of the idea of volumetric growth theory, which we use here.

In the last section we will discuss some results from the study of the form of growth law. We studied the form of growth law for two cases; the simulation of the uniform stress distribution in the ventricle wall (known as residual stress) (see section 4.3.1.) and the simulation of the normal ventricle growth as the case of volume overload (see section 4.3.2.). The simulation was done on the geometry of horizontal cut of the ventricle, for simplicity. We assume only ventricle volume and shape changes, without change in tissue properties - tissue compliance, fibre orientation.

2. Mechanical load of ventricle

2.1. Definition of growth

There exist more definition of the term ”growth”. We are agree with those listed in [5].

*Corresponding author. Tel.: +420 377 632 359, e-mail: mtringel@kme.zcu.cz.

Maintenance - normal programmed or adaptive processes during maturity that consist of a balanced turnover of cells and extracellular matrix at an unchanging configuration or subset of configurations; hence, there is not net change in mass, structure, or properties.

Growth - an increase in mass that is achieved locally via an increase in the number (e.g., via proliferation, *hyperplasia*, or migration) or size (*hypertrophy*) of cells and (or) via a synthesis of extracellular matrix that exceeds removal; growth may or may not change the mass density or material properties.

For simplicity, we are concentrated on a maintenance of the ventricle pumping function, when cell hypertrophy becomes the main growth process.

2.2. Volume and pressure overload

The mechanical load could lead to physiological or pathological adaptation. We assume now only physiologic changes as the result in the differentiation of the right and the left ventricle to the mechanical stimuli after birth on. The main aim of the ventricle adaptation is to preserve its pumping function if there is the increase (decrease) in mechanical load. This effort could be mainly physiological in the first period of life; if the mechanical load increases slowly and gradually, see [3].

The cardiac growth is associated with progressive myocardial cell enlargement (hypertrophy) in some months after birth on. Substantial increases in ventricular diameter and wall thickness result from the addition of new contractile proteins in series and parallel within a virtually constant population of cardiac muscle cells, we refer to [3].

Volume overload. When the ventricular volume overload - the increase of blood volume at the end-diastole - becomes the stimulus, increased fiber stress at the end-diastole leads to series addition of new sarcomeres, fiber elongation and chamber enlargement. The progressive chamber enlargement will lead to increase systolic wall stress, which causes wall thickening to *normalize systolic wall stress*.

Pressure overload. When pressure overload - inner ventricle pressure necessary for blood ejection - becomes the stimulus, the increase in systolic pressure and wall stress leads to the addition of new myofibrils in parallel and wall thickening. *The systolic wall stress will be normalized*.

In [4] there are named more ventricle characteristics which are holt quasi constant during the volume overload. These are the end-diastole fibre strain, systolic wall stress, fibre contraction, etc. We assume in our computer simulation wall stress to be kept constant.

3. Theory of volumetric growth

The theory of volumetric growth in [1] stays on several fundamental points of the theory of generalized continuum, see [2]. The first point of them is the refinement of the process of motion. In classical continuum mechanics is the process of motion introduced by the placement which maps the body $\mathcal{B}$ onto the Euclidean space $\mathcal{E}$

$$p : \mathcal{B} \to \mathcal{E}. \tag{1}$$

If we would like to assume the microstructure from macroscopic point of view, the process of motion must be refine. The added degree of freedom is represented by the tensorial component which could express the gradient matrix (not necessary skew). In the theory of volumetric growth is added the so called growth tensor $\mathbf{P}$, which is characterized as the mapping of the tangential space of body $\mathcal{B}$ onto vectorial Euclidean space $\mathcal{E}$

$$\mathbf{P} : \mathbf{T}_b\mathcal{B} \to \mathbf{V}\mathcal{E}. \tag{2}$$

The refined motion is then given by the process (p, $\mathbf{P}$).

The second point of the here mentioned theory of volumetric growth is theory of gradient order in the construction of the balance laws (balance of forces, growth law). The theory of gradient order is explained in [6]. It is not necessary, that every element of the process be of same gradient order. A first-order gradient theory clearly describes usual continua (called "simple materials") and is, most often, quite sufficient. A first-order gradient theory is applied to the placement p. A zero-order gradient theory is used for the growth tensor $\mathbf{P}$, for simplicity. This choice restricts the theory of volumetric growth only on the growth in mass due to cell enlargement. The placement p and the growth tensor $\mathbf{P}$ are related by

$$\mathbf{F} = \nabla p \mathbf{P}^{-1}, \tag{3}$$

where warp $\mathbf{F}$ preserves the compatibility of growing body, see [7].

Once is chosen the process of motion, the principle of working (principle of virtual power) and the principle of dissipation is used to construct the balance equation and the growth law with corresponding constitutive relation. We assume elastic continuum. For more information see [1].

Balance equation expressed on the relaxed - "stress-free", see [7] - configuration

$$\mathrm{Div}\mathbf{S} = \mathbf{b} \;\; on \;\; \mathcal{B} \;\; \& \;\; \mathbf{S}\mathbf{n}_{\partial\mathcal{B}} = \mathbf{t}_{\partial\mathcal{B}} \;\; \partial\mathcal{B}, \tag{4}$$

where $\mathbf{S}$ is the stress tensor (inner force)[1], $\mathbf{b}$ is the bulk force (outer force), $\mathbf{n}$ is the normal to the boundary of body $\mathcal{B}$ and $\mathbf{t}$ is the boundary force (outer force).

The relation between stress tensor $\mathbf{S}$ expressed on relaxed configuration and stress tensor $\mathbf{T}$ expressed on current configuration (also known as *Cauchy stress tensor*) is given

$$\mathbf{T} = J_{\mathbf{F}}^{-1}\mathbf{S}\mathbf{F}^{\mathrm{T}}, J_{\mathbf{F}} = \mathrm{det}\mathbf{F}. \tag{5}$$

Growth law expressed on the relaxed configuration

$$\mathbb{G}\dot{\mathbf{P}}\mathbf{P}^{-1} = \mathbf{B} - \psi\mathbf{I} + \mathbf{F}^{\mathrm{T}}\mathbf{S} \;\; on \;\; \mathcal{B}, \;\; \mathbf{P}_{t=0} = \mathbf{I}, \tag{6}$$

where $\mathbb{G}$ should be positive-definite matrix of constants (or time variables), see [1], ψ is the free energy, $\mathbf{I}$ is the identity tensor and $\mathbf{B}$ is the couple stress (outer force) which could represent an outer control of the growing process given by implicit processes, chemical processes etc., which are not included directly into the here used model of volumetric growth.

We refer the readers to article [1] to understand the creation of both balance and growth law.

4. Study of form of growth low

4.1. Model of ventricle

The right and the left ventricles have very complicated geometry. For simplicity, we assume that the ventricle could be represented by a prolate spheroid. For our computer simulation we take only very thin horizontal cut from the equatorial plane of prolate spheroid, represented by the geometry of an annulus (R_i = 0.02m - inner radius, R_o = 0.05m - outer radius) , see fig. 1. We solve the problem of plain strain.

[1] The dichotomy inner/outer does not pertain to the physics of forces, but to the limitations of the model.

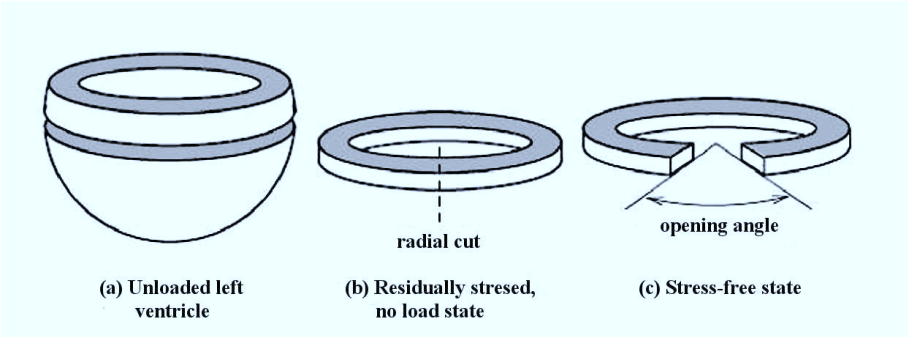

Fig. 1. Horizontal cut from the equatorial plane of prolate spheroid.

Ventricle wall is moulding as incompressible material (7)

$$\mathbf{S} = \mathbf{S}_{ext} - p\mathbf{I}\mathbf{P}^*, {}^2\mathbf{S}_{ext} = 2\mathbf{F}\frac{\partial W(\mathbf{C})}{\partial \mathbf{C}}, {}^3 \tag{7}$$

where p is hydrostatic pressure (don't replace by the notation p for body placement).

We assume the tissue as fiber reinforced material. The constitutive relation used for the simulation is composed from two parts, the first one which represents the matrix and the second one which represents the contractile fibers

$$W(\mathbf{C}) = W_m + W_f = C_1(e^{(a(I_1-3))} - 1) + C_2(e^{(b(\alpha-1)^2)} - 1), \tag{8}$$

where $I_1 = tr\mathbf{C}, \alpha = \mathbf{e} \otimes \mathbf{e} : \mathbf{C}$, a vector $\mathbf{e}$ characterizes the fiber orientation (here only in circumferential direction), $C_1 = 0.001[MPa]$, $C_2 = 1[MPa]$, a = 0.001, b = 1.5 are here used material constants, $\psi = W(\mathbf{C})$ is the strain energy and $\mathbf{C}$ is the deformation measure (called *left Cauchy-Green deformation tensor*).

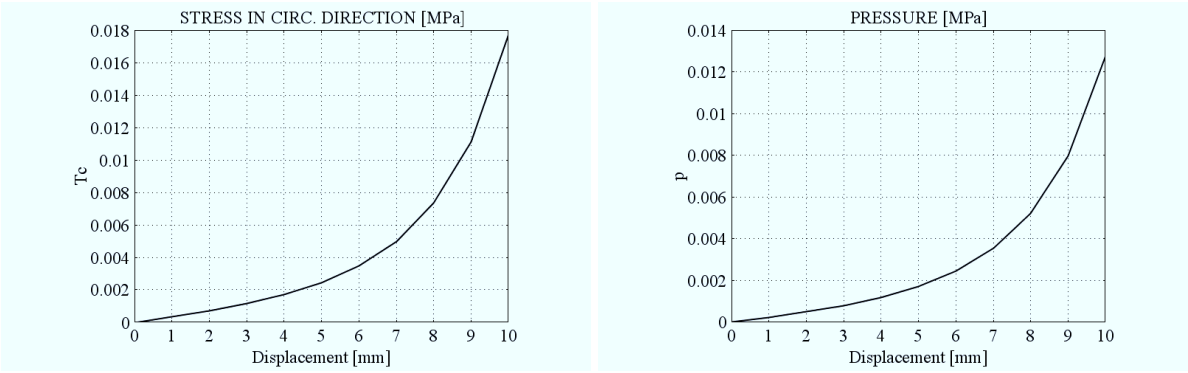

Fig. 2. Dependence of stress in circumferential (fiber) direction ($\mathbf{T}_c$) and inner ventricle pressure p_i to prescribed displacement.

We are interested in the form of matrix $\mathbb{G}$ and tensor $\mathbf{B}$ of relation (6). Matrix $\mathbb{G}$ could express the tissue compliance to adaptation. $\mathbf{B}$ - couple stress - introduces the outer control of adaptation (growth) process. If we assume the growth only in radial (r) and circumferential (c) direction, the relation (6) could be rewritten

[2] $\mathbf{P}^* = \det\mathbf{P}\ \mathbf{P}^{-1}$
[3] $\mathbf{C} = \mathbf{F}\mathbf{F}^{\mathrm{T}}$

$$\mathbb{G}_{11}\frac{\dot{\mathbf{P}}_r}{\mathbf{P}_r}+\mathbb{G}_{12}\frac{\dot{\mathbf{P}}_c}{\mathbf{P}_c}=\mathbf{B}_r-W+\mathbf{F}_r\mathbf{S}_r,$$
$$\mathbb{G}_{21}\frac{\dot{\mathbf{P}}_r}{\mathbf{P}_r}+\mathbb{G}_{22}\frac{\dot{\mathbf{P}}_c}{\mathbf{P}_c}=\mathbf{B}_c-W+\mathbf{F}_c\mathbf{S}_c. \tag{9}$$

4.2. Passive growth

Firstly, we tested the relation (6), if **B** was neglected - *passive growth*. The bulk force **b** was neglected too and the *Dirichlet* boundary condition in (4) was applied. The matrix $\mathbb{G}$ should be positive-definite. We tasted three different cases of $\mathbb{G}$ rewritten into matrix form

$$\mathbb{G}=\begin{bmatrix}\mathbb{G}_{11} & \mathbb{G}_{12}\\ \mathbb{G}_{21} & \mathbb{G}_{22}\end{bmatrix}=a)\begin{bmatrix}1 & 0\\ 0 & 1\end{bmatrix},b)\begin{bmatrix}1 & 0\\ 0 & 10\end{bmatrix},c)\begin{bmatrix}10 & 0\\ 0 & 1\end{bmatrix}. \tag{10}$$

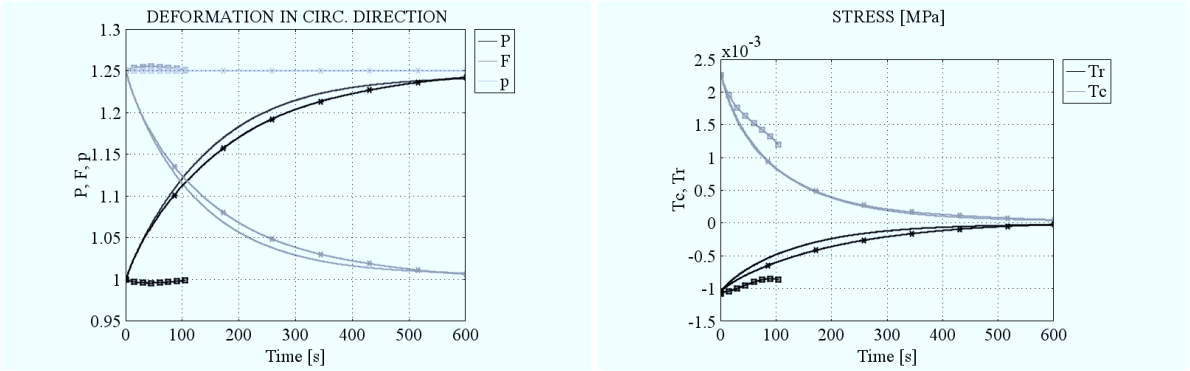

Fig. 3. Time dependence of deformation (P-black, F-dark grey, ∇p - light grey) and stress ($\mathbf{T}_c$ - dark grey, $\mathbf{T}_r$ - black) for $\mathbb{G}$ ((*a*) - solid line, (*b*) - solid line(□), (*c*) - solid line(∗)).

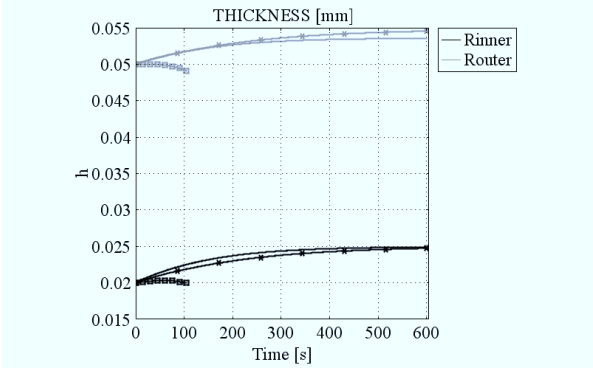

Fig. 4. Time dependence of radius (inner - black, outer - dark grey) for $\mathbb{G}$ ((*a*) - solid line, (*b*) - solid line(□), (*c*) - solid line(∗)).

The compliance to the adaptation - expressed by matrix $\mathbb{G}$ - depends on the value of the components of $\mathbb{G}$. If $\mathbb{G}$ is diagonal matrix; whereby is the diagonal $\mathbb{G}$ component greater thereby is the growth in that direction slower, see fig. 3 right. The case (*b*) stopped, because it did not fulfil the condition of incompressibility $\det\mathbf{F}=1$. If diagonal $\mathbb{G}$ component for both radial and circumferential direction is same (case (*a*)), the annulus becomes thinner for *passive*

growth then in the (case (*c*)), see fig. 4. $\mathbb{G}$ could also depend on the time. This could be useful by the simulation of the ventricle adaptation, when the stimulus to adaptation depends on the different mechanical load in diastole and systole separately.

4.3. Active growth

Secondly, we tested the relation (6), if **B** was taken into account, see (11) - *active growth*. The bulk force **b** was neglected and the *Dirichlet* boundary condition in (4) was applied.

$$\mathbf{B} = W\mathbf{I} - (\det\mathbf{F})\mathbf{F}^{\mathrm{T}}\mathbf{T}^{\odot}\mathbf{F}^{-\mathrm{T}}, \tag{11}$$

where components of $\mathbf{T}^{\odot}$ represent the desired value (control value) of stress in radial $\mathbf{T}^{\odot}_r$ and circumferential $\mathbf{T}^{\odot}_c$ direction, if we consider the plain strain problem and the growth only in radial and circumferential direction. If we assume the relation (11), then the relations (9) could be rewritten

$$\begin{aligned}
\mathbb{G}_{11}\frac{\dot{\mathbf{P}}_r}{\mathbf{P}_r} + \mathbb{G}_{12}\frac{\dot{\mathbf{P}}_c}{\mathbf{P}_c} &= \mathbf{F}_r(\mathbf{T}_r - \mathbf{T}^{\odot}_r)\mathbf{F}_r,\\
\mathbb{G}_{21}\frac{\dot{\mathbf{P}}_r}{\mathbf{P}_r} + \mathbb{G}_{22}\frac{\dot{\mathbf{P}}_c}{\mathbf{P}_c} &= \mathbf{F}_c(\mathbf{T}_c - \mathbf{T}^{\odot}_c)\mathbf{F}_c.
\end{aligned} \tag{12}$$

4.3.1. Uniform wall stress

The stress in fiber (here circumferential) direction was observed to be uniform at the end-diastole [8]. This even was observed on the horizontal cut of the ventricle, the ring opened if it was cut radially, see fig. 1.

We simulated tree different cases, which could lead to the uniformity of stress in circumferential direction controlled by

$$\mathbf{T}^{\odot} = \begin{bmatrix} \mathbf{T}^{\odot}_r & 0 \\ 0 & \mathbf{T}^{\odot}_c \end{bmatrix} = a) \begin{bmatrix} \mathbf{T}_r & 0 \\ 0 & p_i\frac{R_i}{R_o - R_i} \end{bmatrix}, \tag{13}$$

where $p_i\frac{R_i}{R_o-R_i}$ is Laplace law for thin walled annulus, p_i is the inner ventricle pressure.

The first (1) case represents the possibility, that the tissue growths only in circumferential direction. The second (2) case expresses the growth both in circumferential and radial direction. The third (3) case simulates the growth in circumferential direction and the atrophy in radial direction. The matrix $\mathbb{G}$ should be positive-definite. We tasted three different cases of $\mathbb{G}$ rewritten into matrix form

$$\mathbb{G} = \begin{bmatrix} \mathbb{G}_{11} & \mathbb{G}_{12} \\ \mathbb{G}_{21} & \mathbb{G}_{22} \end{bmatrix} = 1) \begin{bmatrix} 1 & 0 \\ 0 & 1 \end{bmatrix}, 2) \begin{bmatrix} 1 & -0.5 \\ -0.5 & 1 \end{bmatrix}, 3) \begin{bmatrix} 1 & 0.5 \\ 0.5 & 1 \end{bmatrix}. \tag{14}$$

We show in the following figures the difference in the radial $\mathbf{P}_r$ and the circumferential $\mathbf{P}_c$ growth, the angle opening, the change of wall thickness h, the stress in the radial $\mathbf{T}_r$ (cross fiber) direction and the pass to the uniform stress in the circumferential $\mathbf{T}_c$ (fiber) direction for inner (black line) and outer (grey line) radius of the annulus. The time of simulation was $t \in \langle 0, 600\rangle[s]$. Case (1) is represented by solid line, case (2) by solid line $*$, and case (3) by solid line $\square$.

We observed the differences in the geometry proportions for these three cases. These differences lead to the different inner ventricle pressure after the circumferential stress became

uniform across the wall. At the time $t = t_0 = 0$ is shown in fig. 5 the difference between the fiber (circumferential) stress (grey line) across the wall and control value (black line).

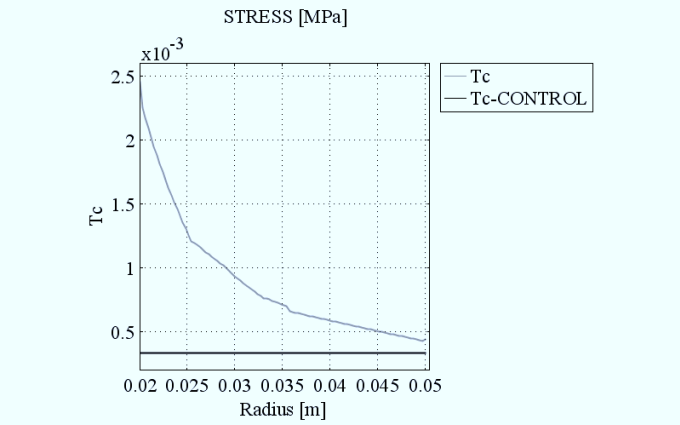

Fig. 5. Initial difference between fiber stress and control value across the wall.

The stress in fiber (circumferential) direction T_c, see fig. 6 left, passed to the control value at the time of simulation $t = 600s$. In the case (3) (□ line) was the passing the fastest for both inner (black line) and outer (grey line) radius. In the case (2) was the passing the slowest for the outer radius (grey line $*$). In all three cases, the difference in stress in cross-fiber (radial) direction T_r, see fig. 6 right, for inner radius (black line) expresses the difference in inner ventricle pressure after the circumferential stress became uniform across the wall - at time $t = 600s$. For the outer radius (grey line) there is no change in the stress in radial direction, the outer boundary is free to move.

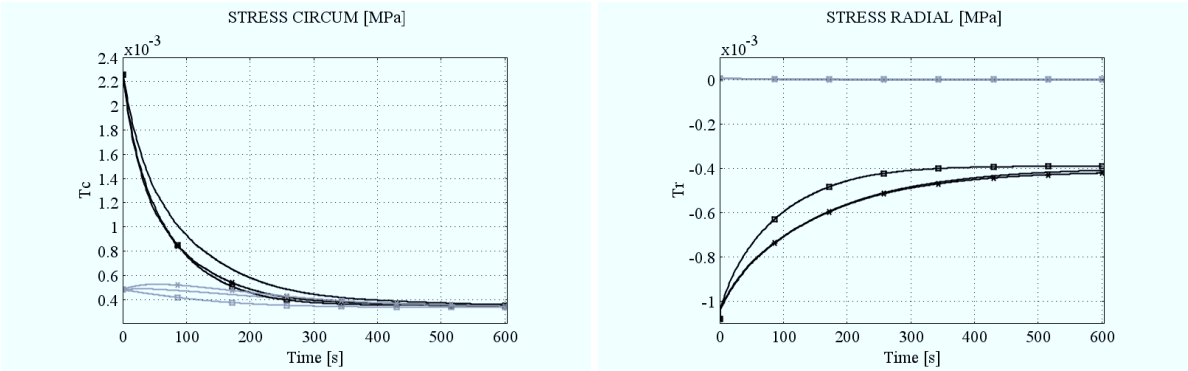

Fig. 6. Simulation of the fiber stress uniform distribution across the wall - left figure, and change in the radial stress for the inner radius (black line) - right figure.

The difference in the inner ventricle pressure for three cases will be better shown in the following figures. If we have in mind the Laplace law for thin walled vessel (15)

$$\mathrm{T}_c = p_i \frac{R_i}{R_o - R_i}, \tag{15}$$

if T_c is constant, then the value of the inner ventricle pressure p_i depends on the relation of the inner R_i and the outer R_o radius $\frac{R_i}{R_o - R_i}$.

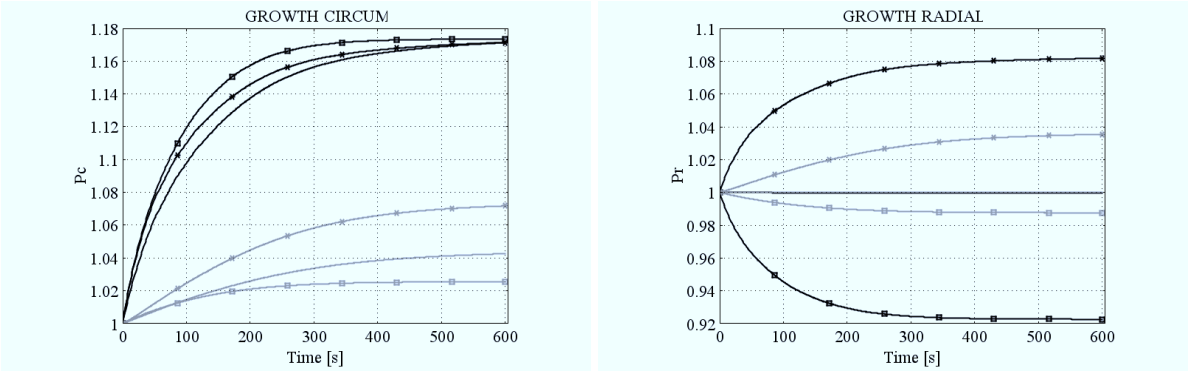

Fig. 7. Growth in circumferential P_c and radial P_r direction for three cases. Inner radius (black line), outer radius (grey line).

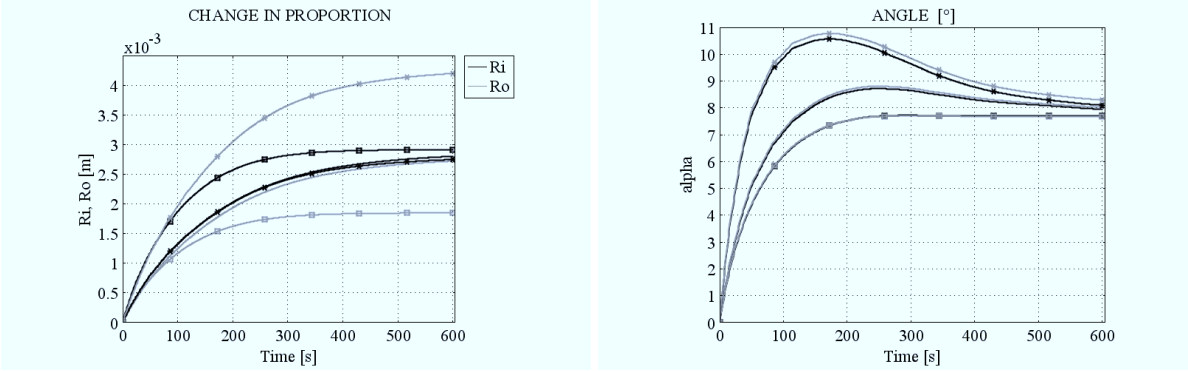

Fig. 8. Left fig. - Change of inner radius R_i (black line), outer radius R_o (grey line). Right fig. - Time evolution of angle opening for inner radius (black line), outer radius (grey line).

After simulation when the stress in circumferential direction became uniform:

Case 1 - solid line. The inner radius R_i increased about the value $2.7mm$ but the wall thickness $R_0 - R_i$ did not change. The inner pressure must decrease (see fig. 6 right - opposite value to T_r for inner radius (black solid line)).

Case 2 - solid line $*$. The inner radius R_i changed as in case 1. The outer radius increased significantly about the value $4.3mm$, so the wall thickness $R_0 - R_i$ increased. The inner ventricle pressure decreased less then in the case 1 (see fig. 6 right (black solid line $*$)).

Case 3 - solid line $\square$. The outer radius R_0 changed about the value $2.9mm$. The inner radius increased less then in case 1 about the value $1.8mm$, so the wall thickness increased with the smaller inner radius. This leads to the greater decrease in the inner ventricle pressure then in case 1 (see fig. 6 right (black solid line $\square$)).

The opening of radial cut of the annulus is shown by the time simulation of angle $\alpha[^\circ]$, see fig. 8 right. The difference in time $t = 100s$ depends on the difference in growth in circumferential direction P_c, see fig. 7 left, and change in proportion, see fig. 8 left. At time $t = 100s$ there are no significant changes in proportions for both three cases, but the difference in the growth in circumferential direction is significant. At the end of simulation the opening angle stops nearly on the same value around 8°.

4.3.2. Normal growth

The lass computer simulation is dedicated to the normal growth of the left ventricle. The adaptation on the increase in both volume and pressure load after birth on leads to normalize *systolic wall stress*, which is necessary for valve opening and blood ejection [3]. The pressure in the ventricle must achieve the value of the pressure in artery during the isovolumic systole. The end-diastole sarcomere length should be kept constant; equal to the value 2.2μm which is an optimal sarcomere length for its contraction. We simulate the normal growth in two steps.

The first step (time of simulation $t \in \langle 0, 600 \rangle$ [s]) simulates the passing of stress in the circumferential direction on the constant value (uniform stress distribution in circumferential direction at the end-diastole) which could represent the uniform optimal sarcomere length in the wall. The first step is same as in section 4.3.1case (1). The tissue growth only in circumferential direction.

The second step (time of simulation $t \in \langle 600, 3000 \rangle$ [s]) simulates the achievement of constant value of inner pressure. The stress in circumferential direction and the inner radius are holt constant in the second step, equal to the value reached in the first step. The stress in radial direction $\mathbf{T}_r$ passes to the control value $\mathbf{T}_r^{\odot}$, see fig. 9.

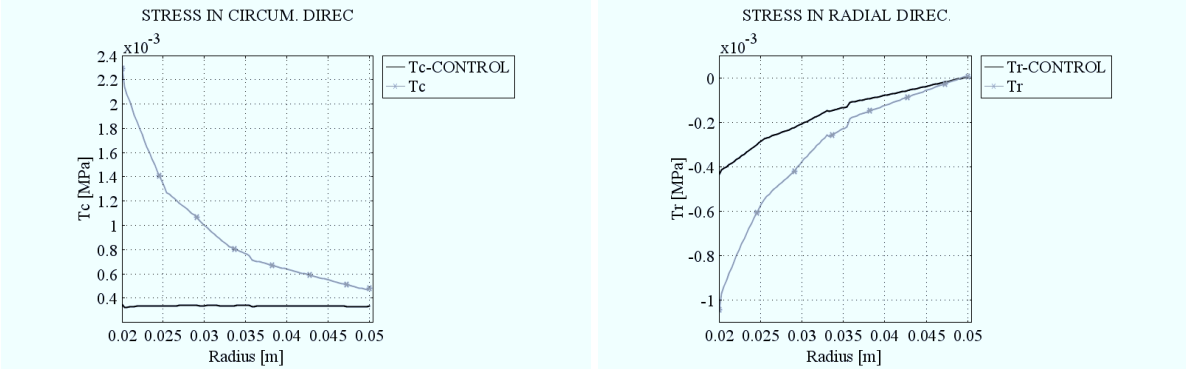

Fig. 9. Initial conditions for stress in circumferential direction for 1^{th} step of simulation (left figure) and radial direction for 2^{nd} step of simulation (right figure)(grey solid line $*$), control value (black solid line).

The following figures (on the next page) show the time evolution of the stress in circumferential direction and inner ventricle pressure. The tissue responds to the increase in end-diastole volume and efforts to balance the inner vessel pressure on the control value by the credit of the change in inner and outer radius of the annulus. The calculations served only as a model. The parameters used for the simulation were not real.

5. Conclusion

The contents of this work was the study of the form of growth low which we will used in future for the computer simulation of left ventricle adaptation to the mechanical stimuli. The response of tissue (here represented by fiber reinforced annulus) on the mechanical load, which is driven by here studied growth low, depends on the form of both $\mathbb{G}$ matrix and $\mathbf{B}$ couple stress. We could conclude that the velocity of growth process depends on the compliance to the growth - expressed by $\mathbb{G}$ matrix, while $\mathbf{B}$ couple stress drives the growth to desire values (here the value of uniform stress in circumferential direction). The initial calculation was done on the geometry of the annulus. The simulation for the model of prolate spheroid with helical fiber orientation is still in progress.

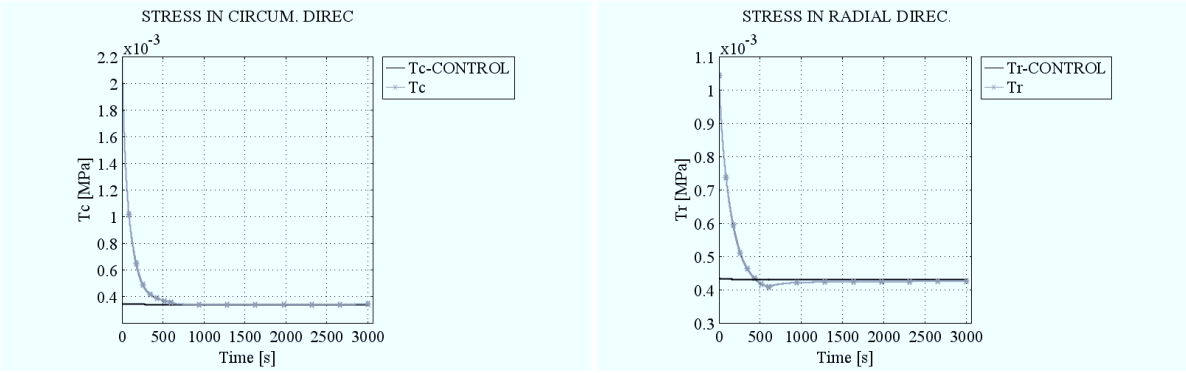

Fig. 10. Passing of stress in circumferential direction (grey solid line $*$) on constant value (left figure) and balance of inner ventricle pressure (grey solid line $*$) on control value (right figure).

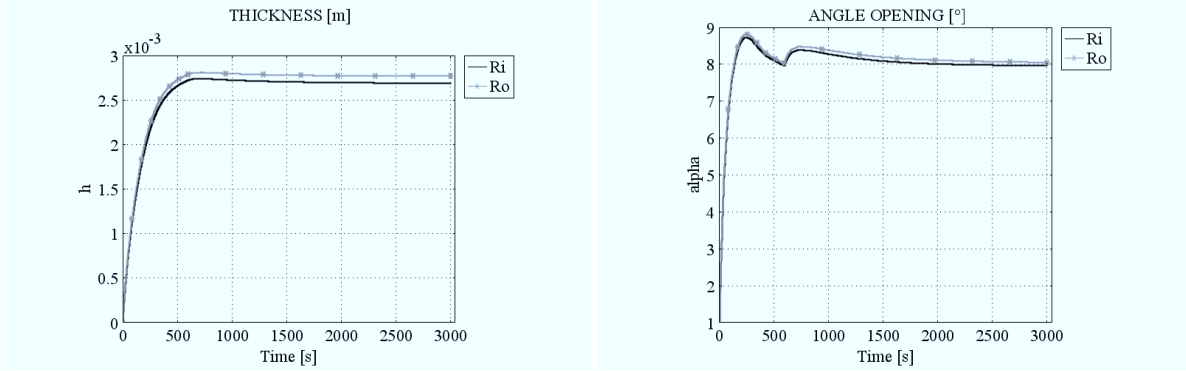

Fig. 11. Time evolution of inner (black solid line) and outer (grey solid line $*$) radius and angle opening for inner (black solid line) and outer (grey solid line $*$) radius.

Acknowledgements

The work has been supported by the research project MSM 4977751303.

References

[1] A. DiCarlo, S. Quiligotti, Growth and balance, Mechanics Research Communications 29 (2002) 449-456.

[2] P. Germain, The method of virtual power in continuum mechanics. Part 2: Microstructure, SIAM Journal on Applied Mathematics 25 (3) (1973) 556-575.

[3] W. Grossman, Cardiac hypertrophy: Useful adaptation or pathologic process? The American Journal of Medicine 69 (1980) 576-584.

[4] J.F. Holmes, Candidate mechanical stimuli for hypertrophy during volume overload, Journal of Applied Physiology 97 (2004) 1456-1460.

[5] J.D. Humphrey, K.R. Rajagopal, A constrained mixture model for growth and remodeling of soft tissues, Mathematical Models and Methods in Applied Sciences 12 (3) (2002) 407-430.

[6] G.A. Maugin, The method of virtual power in continuum mechanics: Application to coupled fields, Acta Mechanica 35 (1980) 1-70.

[7] E.K. Rodriguez, A. Hoger, A.D. McCulloch, Stress dependent finite growth in soft elastic tissues, Journal of Biomechanics 27 (4) (1994) 455-467.

[8] B.B. Šrámek, J. Valenta, F. Klimeš, Biomechanics of the cardiovascular system, Czech Technical University Press, 1995.